Inorganic Chemistry

Communication

pubs.acs.org/IC

Why So Slow? Mechanistic Insights from Studies of a Poor Catalyst for Polymerization of ε-Caprolactone

Daniel E. Stasiw, Mukunda Mandal, Benjamin D. Neisen, Lauren A. Mitchell, Christopher J. Cramer,* and William B. Tolman*

Department of Chemistry, Center for Sustainable Polymers, Chemical Theory Center, and Minnesota Supercomputing Institute (MSI), University of Minnesota, 207 Pleasant Street SE, Minneapolis, Minnesota 55455, United States

Supporting Information

ABSTRACT: Polymerization of ε-caprolactone (CL) using an aluminum alkoxide catalyst (**1**) designed to prevent unproductive trans binding was monitored at 110 °C in toluene-d_8 by ^{1}H NMR and the concentration versus time data fit to a first-order rate expression. A comparison of $t_{1/2}$ for **1** to values for many other aluminum alkyl and alkoxide complexes shows much lower activity of **1** toward polymerization of CL. Density functional theory calculations were used to understand the basis for the slow kinetics. The optimized geometry of the ligand framework of **1** was found indeed to make CL trans binding difficult: no trans-bound intermediate could be identified as a local minimum. Nor were local minima for cis-bound precomplexes found, suggesting a concerted coordination−insertion for polymer initiation and propagation. The sluggish performance of **1** is attributed to a high-framework distortion energy required to deform the "resting" ligand geometry to that providing optimal catalysis in the corresponding transition-state structure geometry, thus suggesting a need to incorporate ligand flexibility in the design of efficient polymerization catalysts.

Understanding the mechanism(s) of the ring-opening transesterification polymerization (ROTEP) of lactones by metal alkoxide complexes is a key prerequisite for the rational design of catalysts for the synthesis of sustainable polymers.[1] In recent studies, we were able to dissect the paradigm coordination−insertion mechanism into monomer binding equilibrium (K_{eq}) and insertion (k) steps through the observation of saturation kinetics in the ROTEP of ε-caprolactone (CL) by aluminum salen complexes (Figure 1).[2,3] In one case, we hypothesized that the observed kinetics were affected by unproductive, inhibitory binding of monomer trans to the metal alkoxide moiety.[2c] Inhibition was supported by theoretical calculations, which identified a trans-bound intermediate as a low-energy stationary point. Reasoning that if such trans binding could be prevented, inhibition would be obviated and the ROTEP rate would be increased, we considered how ligand modifications might be implemented that would hinder unproductive monomer coordination. Simple strategies of increasing the steric bulk of salens generally affect interactions cis to the metal alkoxide bond and prevent catalyst dimerization but do not necessarily preclude unproductive binding, thus leading us to consider alternative ligand designs.[4]

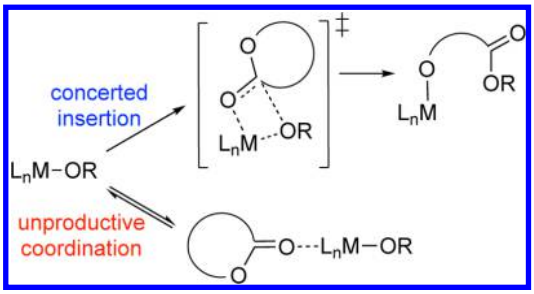

Figure 1. Concerted coordination−insertion ROTEP showing both productive (above) and unproductive (below) mechanistic pathways.

As one strategy, we searched for a tetradentate supporting ligand that would cause the trans position to the metal alkoxide to be sterically inaccessible to the monomer yet would retain a five-coordinate geometry and, we reasoned, potentially high reactivity toward ROTEP. The nonplanar structure of tetramethyl-5,7,12,14-dibenzo-1,4,8,11-tetraaza[14]annulene (TMTAA) in aluminum complexes offered promise because of its demonstrated tendency to induce protrusion of the metal center ∼0.54 Å above the ligand donor plane, thus disfavoring trans coordination of a sixth ligand.[5] Similar metal protrusions have been seen with porphyrins in metal−μ-oxo−metal[6] and metal alkyl[7] complexes. Additionally, controlled reactivity of aluminum alkoxide porphyrin complexes toward the polymerization of CL indicated the promise of high reactivity in the similar ligand environment provided by TMTAA.[8] While aluminum chloride complexes of both TMTAA and porphyrins have been used to control steric bulk around the catalytic center for epoxide ring-opening polymerizations,[9] we found no examples of the use of TMTAA−aluminum complexes for the catalytic ROTEP of cyclic esters. Herein, we report the synthesis and characterization of (TMTAA)AlOEt and its exploration as a catalyst for ROTEP of CL. Surprisingly, this five-coordinate aluminum alkoxide is a very sluggish catalyst, a "negative" result, but one from which we were able to learn valuable lessons through further analysis of the reaction mechanism and associated potential energy surface using density functional theory (DFT).

Experimental Results. Reaction of the known[8] compound (TMTAA)AlCl with NaOEt at 70 °C in tetrahydrofuran yielded (TMTAA)AlOEt (**1**, 84%), which was characterized by ^{1}H and ^{13}C NMR spectroscopy and X-ray crystallography (Figure 2).

Received: November 27, 2016
Published: December 22, 2016

DOI: 10.1021/acs.inorgchem.6b02849
Inorg. Chem. 2017, 56, 725−728

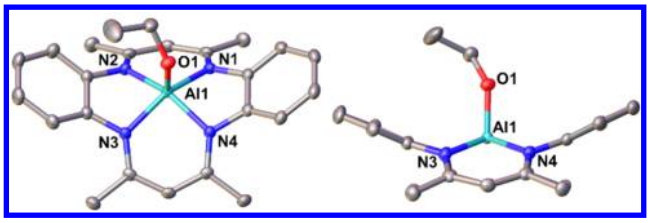

Figure 2. Top-down (left) and side-on (right) views of the X-ray structure of **1**, with H atoms hidden for clarity and other atoms shown as 50% thermal ellipsoids. Selected interatomic distances (Å) and angles (deg): Al1−N1, 1.9556(10); Al1−N2, 1.9446(10); Al1−N3, 1.9463(10); Al1−N4, 1.9374(10), Al1−O1, 1.7325(9); N1−Al1−N2, 89.96(4); N2−Al1−N3, 81.68(4); N3−Al1−N4, 90.60(4); N4−Al1−N1, 81.78(4); O1−Al1−N1, 105.80(4); O1−Al1−N2, 108.00(4); O1−Al1−N3, 105.37(5); O1−Al1−N4, 101.96(4).

The monomeric, five-coordinate complex adopts a square-pyramidal geometry at the Al center (τ = 0.02, where τ = 0 is square pyramidal and τ = 1 is trigonal bipyramidal)[10] with the metal center displaced 0.51 Å above a plane created by the N atoms of the annulene ring. The displacement of the Al atom and the geometry of the puckered annulene ring closely resembles those of other aluminum complexes reported previously.[5,8]

Polymerizations of CL using complex **1** were performed in duplicate with fixed concentrations of CL (0.8 M < $[CL]_0$ < 2 M) and catalyst (8 mM < $[\mathbf{1}]_0$ < 20 mM) in toluene-d_8 at 110 °C. ^{1}H NMR features specific to the growth of polymer and decay of monomer in the polymerizations were monitored to polymerization completion (>95% conversion) using 4 mM 1,4-bis(trimethylsilyl)benzene as an internal standard. The concentration versus time data for the CL polymerization were fit with COPASI[11] to the first-order rate expression of rate = $k_{obs}[CL]$, where k_{obs} is the rate constant for polymer propagation (illustrative plot shown in Figure 3). From this analysis, k_{obs} = 3.6(5) × 10^{-4} min^{-1}, which corresponds to $t_{1/2}$ = 1920 min. Poly(ε-caprolactone) was isolated from these kinetic experiments via precipitation in cold methanol. The solids were dried under reduced pressure, and size-exclusion chromatography using a dynamic light scattering detector revealed the average molecular weight (M_w = 15.06 kDa) and dispersity ($Đ$ = 1.99) of the resulting polymer. We surmise that the poor dispersity is a consequence of transesterification reactions that occur over the very long reaction time.

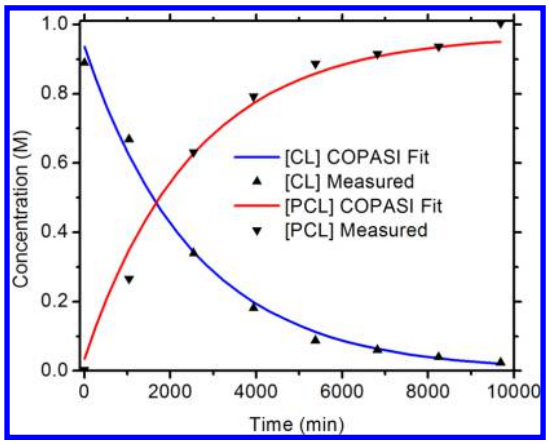

Figure 3. Concentration versus time profile for the ^{1}H NMR resonance decay of CL (▲) and the growth of PCL (▼) along with the fits (blue and red lines) determined by COPASI for $[CL]_0$ = 1 M.

In order to provide context to the rate of ROTEP of CL with **1**, it is helpful to analyze ROTEP rates for other reported aluminum alkoxide and alkyl complexes. The selected complexes shown in Figure 4 showcase the range of rates observed, with a comprehensive list of reported complexes, rates, and reaction conditions given in Table S2. While a comparison of the rates between complexes under different conditions can be problematic, an approximate comparison can be made through calculated $t_{1/2}$ values from reported experimental rate constants. Of this selection, **2**[2c] ($t_{1/2}$ = 0.006 min) and **3**[12] ($t_{1/2}$ = 10 min) represent, on average, some of the faster rates reported for aluminum complexes, while **4**[12] ($t_{1/2}$ = 104 min) and **5**[13] ($t_{1/2}$ = 332 min) are some of the slower catalysts. Note that the range of $t_{1/2}$ values is over ~5 orders of magnitude just for this selection. Complex **1** polymerizes CL ~ 6 times slower than **5** (for **1**, $t_{1/2}$ = 1920 min). We are unaware of any reports of catalysts with rates as slow as **1**. With so many aluminum alkyl and alkoxide complexes polymerizing CL within shorter time frames, we sought to investigate through calculation what causes **1** to be particularly inactive toward ROTEP of CL.

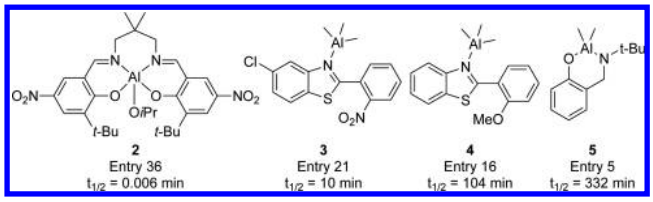

Figure 4. Selected aluminum alkyl and alkoxide complexes from Table S2 representing the range of rates reported for ROTEP of CL.

Theoretical Modeling. To gain insight into the inactivity of **1** in catalyzing CL homopolymerization, DFT was employed, and the energetics of key intermediates and transition-state (TS) structures involved during CL-to-PCL conversion were determined.[14] For computational efficiency, the original aluminum ethoxide complex (**1**, [Al]-OEt) was modeled as an aluminum methoxide (**1′** [Al]-OMe; Scheme 1). Owing to the geometry of the TMTAA ligand and the displacement of the Al atom above the donor ligand plane in **1** (Figure 2), we hypothesized that CL would not bind the Al center in a trans fashion. Indeed, we could not locate an energy minimum on the potential energy surface involving CL bound trans to the [Al]−OMe bond (other than trivial van der Waals complexes having no atoms within the bonding distance of the "open" Al site). In this respect, our initial design goal was successful, and we expected **1** to show improved catalytic activity compared to, say, aluminum salen complexes like **6**,[2b,c] where inhibitive trans binding reduces the activity (Scheme 1).

Scheme 1. (TMTAA)AlOMe (1′) and Aluminum Salen Complex 6

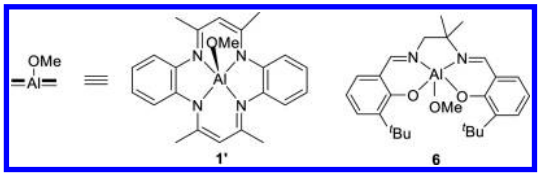

Further analysis of the potential energy surface, however, revealed that the 333 K free energy of activation ($\Delta G^{\ddagger}$) associated with the TS structure for nucleophilic attack of methoxide at the carbonyl C atom of CL [rate-determining step

DOI: 10.1021/acs.inorgchem.6b02849
Inorg. Chem. 2017, 56, 725−728

(RDS) TS1 in Scheme 2] was quite high (30.5 kcal/mol; Figure 5; cf. 14.9 kcal/mol for **6**) consistent with the sluggish activity of **1**.

Scheme 2. Key Stationary Points along the CL ROTEP Reaction Coordinate

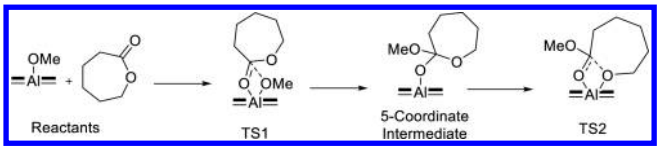

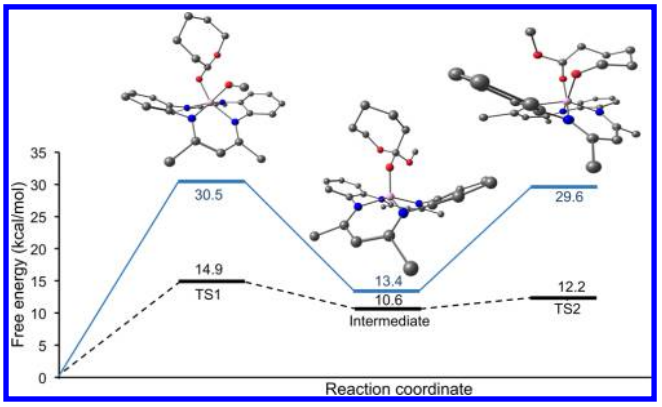

Figure 5. Comparison of the reaction coordinates for 333 K CL ROTEP catalyzed by **1′** (blue solid line) and **6** (black dotted line).[2b] All values were computed at the SMD(toluene)/M06-2X/6-311+G(d,p)//M06-L/6-31+G(d,p) level.[15−19]

In addition to there being no stationary point(s) corresponding to binding of CL trans to the initiating alkoxide, neither could we find any initial six-coordinate precomplexes with CL bound to aluminum cis to the alkoxide, as has been seen in some other aluminum alkoxide complexes[2] (there is a simple van der Waals complex having a 333 K free energy 2.5 kcal/mol above the separated reactants, but because such a species is kinetically irrelevant, we do not consider it further). This suggests a concerted encounter/insertion mechanism followed by ring opening for polymer initiation and propagation, as detailed in Scheme 2 and Figure 5.

To explain the high activation free energy associated with the RDS, we assessed the "framework distortion energy"[2c] associated with **1′**, which measures the energy required to distort a "resting" precatalyst structure to its corresponding TS structure in the absence of reacting ligands. Thus, the framework distortion energy is computed as the difference in the electronic energies of the frozen cationic aluminum-ligand complexes derived from the removal of methoxy from optimized **1′** and methoxy and CL from optimized TS1. The value computed for **1′** is 22.6 kcal/mol, which may be compared to 18.3 kcal/mol for **6**.[2c]

While the difference in these two framework distortion energies is considerably smaller than the difference in the activation free energies, we assign the remainder of the very high free energy of activation for **1′** to the failure of the TMTAA ligand distortion that *does* occur to adequately open a reactive site at the Al atom. Thus, in our prior analysis of the framework distortion energies,[2c] we found that, for a series of eight aluminum salen complexes, all of the equivalent valence bond angles subtended at aluminum in the rate-determining TS structures were identical to within about 2°. Moreover, the X−Al−Y angles for all pairs of cis atoms X and Y derived from the salen ligands were between 85 and 95°; i.e., the geometries in the TS structures were rendered very nearly octahedral when considering the addition of reacting methoxide and CL carbonyl O atoms. By contrast, in TS1 for **1′**, the ligand is unable to distort sufficiently to support such an octahedral geometry (one relevant N−Al−N angle is 125.7°; Figure S4), thereby exposing relatively little of the Al atom to the approaching CL and forcing the nucleophilic attack to proceed with limited activation of the carbonyl. Evidently, though, the energy penalty to *further* distort the TMTAA ligand exceeds the additional catalytic energy lowering that would be associated with a better exposed Al atom.[20]

In conclusion, we learned a key lesson through the study of the slow catalyst **1**. Our work suggests that for future catalyst design, attention must be paid not only to eliminating inhibitory trans binding opportunities but also to constructing ligand frameworks with sufficient flexibility that approximately octahedral TS structures can be accessed at low energetic cost.

■ ASSOCIATED CONTENT

Supporting Information

The Supporting Information is available free of charge on the ACS Publications website at DOI: 10.1021/acs.inorgchem.6b02849.

Experimental data, comparative table of catalyst rates and conditions, and theory details (PDF)

X-ray crystallographic data in CIF format (CIF)

■ AUTHOR INFORMATION

Corresponding Authors

*E-mail: cramer@umn.edu (C.J.C.). Twitter: @ChemProfCramer.

*E-mail: wtolman@umn.edu (W.B.T.). Twitter: @WBTolman.

ORCID

Christopher J. Cramer: 0000-0001-5048-1859

William B. Tolman: 0000-0002-2243-6409

Notes

The authors declare no competing financial interest.

■ ACKNOWLEDGMENTS

Funding for this project was provided by the Center for Sustainable Polymers at the University of Minnesota, a National Science Foundation (NSF)-supported Center for Chemical Innovation (Grant CHE-1413862). The X-ray diffraction experiments were performed using a crystal diffractometer acquired through NSF-MRI Award CHE-1229400. The authors acknowledge the MSI at the University of Minnesota for providing resources that contributed to the research results reported within this paper.

■ REFERENCES

(1) (a) Arbaoui, A.; Redshaw, C. Metal catalysts for ϵ-caprolactone polymerisation. *Polym. Chem.* **2010**, *1*, 801. (b) Kiesewetter, M. K.; Shin, E. J.; Hedrick, J. L.; Waymouth, R. M. Organocatalysis: Opportunities and challenges for polymer synthesis. *Macromolecules* **2010**, *43*, 2093−2107. (c) Wu, J.; Yu, T. L.; Chen, C. T.; Lin, C. C. Recent developments in main group metal complexes catalyzed/initiated polymerization of lactides and related cyclic esters. *Coord. Chem. Rev.* **2006**, *250*, 602−626. (d) Dechy-Cabaret, O.; Martin-Vaca, B.; Bourissou, D. Controlled ring-opening polymerization of lactide and glycolide. *Chem. Rev.* **2004**, *104*, 6147−6176.

DOI: 10.1021/acs.inorgchem.6b02849
Inorg. Chem. 2017, 56, 725−728

(2) (a) Ding, K.; Miranda, M. O.; Moscato-Goodpaster, B.; Ajellal, N.; Breyfogle, L. E.; Hermes, E. D.; Schaller, C. P.; Roe, S. E.; Cramer, C. J.; Hillmyer, M. A.; Tolman, W. B. Roles of Monomer Binding and Alkoxide Nucleophilicity in Aluminum-Catalyzed Polymerization of ε-Caprolactone. *Macromolecules* **2012**, *45*, 5387−5396. (b) Miranda, M. O.; Deporre, Y.; Vazquez-Lima, H.; Johnson, M. A.; Marell, D. J.; Cramer, C. J.; Tolman, W. B. Understanding the Mechanism of Polymerization of ε-Caprolactone Catalyzed by Aluminum Salen Complexes. *Inorg. Chem.* **2013**, *52*, 13692−13701. (c) Marlier, E. E.; Macaranas, J. A.; Marell, D. J.; Dunbar, C. R.; Johnson, M. A.; DePorre, Y.; Miranda, M. O.; Neisen, B. D.; Cramer, C. J.; Hillmyer, M. A.; Tolman, W. B. Mechanistic Studies of ε-Caprolactone Polymerization by (salen)AlOR Complexes and a Predictive Model for Cyclic Ester Polymerizations. *ACS Catal.* **2016**, *6*, 1215−1224.

(3) Selected other examples of CL polymerization by aluminum salen or related complexes: (a) Pepels, M. P. F.; Bouyahyi, M.; Heise, A.; Duchateau, R. Kinetic investigation on the catalytic ring-opening (co)polymerization of (macro)lactones using aluminum salen catalysts. *Macromolecules* **2013**, *46*, 4324−4334. (b) Huang, H.-C.; Wang, B.; Zhang, Y.-P.; Li, Y.-S. Bimetallic aluminum complexes with cyclic β-ketiminato ligands: the cooperative effect improves their capability in polymerization of lactide and ε-caprolactone. *Polym. Chem.* **2016**, *7*, 5819−5827. (c) Kan, C.; Ma, H. Copolymerization of l-lactide and ε-caprolactone catalyzed by mono- and dinuclear salen aluminum complexes bearing bulky 6,6′-dimethylbipheyl-bridge: random and tapered copolymer. *RSC Adv.* **2016**, *6*, 47402−47409. (d) Pappalardo, D.; Annunziata, L.; Pellecchia, C. Living ring-opening homo- and copolymerization of ε-caprolactone and L- and D, L-lactides by dimethyl(salicylaldiminato)aluminum compounds. *Macromolecules* **2009**, *42*, 6056−6062.

(4) (a) Aluthge, D. C.; Yan, E. X.; Ahn, J. M.; Mehrkhodavandi, P. Role of Aggregation in the Synthesis and Polymerization Activity of SalBinap Indium Alkoxide Complexes. *Inorg. Chem.* **2014**, *53*, 6828−6836. (b) Aluthge, D. C.; Ahn, J. M.; Mehrkhodavandi, P. Overcoming Aggregation in Indium Salen Catalysts for Isoselective Lactide Polymerization. *Chem. Sci.* **2015**, *6*, 5284−5292. (c) Nomura, N.; Ishii, R.; Akakura, M.; Aoi, K. Stereoselective Ring-Opening Polymerization of Racemic Lactide Using Aluminum-Achiral Ligand Complexes: Exploration of a Chain-End Control Mechanism. *J. Am. Chem. Soc.* **2002**, *124*, 5938−5939.

(5) Goedken, V. L.; Ito, H.; Ito, T. An Unusually Stable Aluminium-Alkyl Bond: Synthesis and Reactivity Studies of the Macrocyclic Al($C_{22}H_{22}N_4$)Et Complex. *J. Chem. Soc., Chem. Commun.* **1984**, *1*, 1453−1454.

(6) Yamamoto, G.; Nadano, R.; Satoh, W.; Yamamoto, Y.; Akiba, K. Synthesis of μ-oxo-bridged group 15 element − aluminium heterodinuclear porphyrins [(oep) (Me)M−O−Al(oep)]ClO_4 (M = P, As, Sb) and X-ray crystal structure of [(oep) (Me)As−O−Al(oep)]ClO_4. *Chem. Commun.* **1997**, *4*, 1325−1326.

(7) (a) Guilard, R.; Zrineh, A.; Tabard, A.; Endo, A.; Han, B. C.; Lecomte, C.; Souhassou, M.; Habbou, A.; Ferhat, M.; Kadish, K. M. Synthesis and Spectroscopic and Electrochemical Characterization of Ionic and σ-Bonded Aluminum(III) Porphyrins. Crystal Structure of Methyl(2,3,7,8,12,13,17,18-octaethylporphinato)aluminum(III), (OEP)Al(CH_3). *Inorg. Chem.* **1990**, *29*, 4476−4482. (b) Guilard, R.; Barbe, J.-M.; Ibnlfassi, A.; Zrineh, A.; Adamian, V. A.; Kadish, K. M. Synthesis, Characterization, and Electrochemistry of Heteroleptic Double-Decker Complexes of the Type Phthalocyaninato-Porphyrinato-Zirconium(IV) or -Hafnium(IV). *Inorg. Chem.* **1995**, *34*, 1472−1481.

(8) Endo, M.; Aida, T.; Inoue, S. Immortal Polymerization of ε-Caprolactone Initiated by Aluminum Porphyrin in the Presence of Alcohol. *Macromolecules* **1987**, *20*, 2982−2988.

(9) Sugimoto, H.; Kawamura, C.; Kuroki, M.; Aida, T.; Inoue, S. Lewis Acid-Assisted Anionic Ring-Opening Polymerization of Epoxide by the Aluminum Complexes of Porphyrin, Phthalocyanine, Tetraazaannulene, and Schiff Base as Initiators. *Macromolecules* **1994**, *27*, 2013−2018.

(10) Addison, A. W.; Rao, T. N.; Reedijk, J.; van Rijn, J.; Verschoor, G. C. Synthesis, Structure, and Spectroscopic Properties of Copper(II) Compounds containing Nitrogen−Sulphur Donor Ligands; the Crystal and Molecular Structure of Aqua[1,7-bis(*N*-methylbenzimidazol-2′-yl)-2,6-dithiaheptane]copper(II) Perchlorate. *J. Chem. Soc., Dalton Trans.* **1984**, 1349−1356.

(11) Hoops, S.; Sahle, S.; Gauges, R.; Lee, C.; Pahle, J.; Simus, N.; Singhal, M.; Xu, L.; Mendes, P.; Kummer, U. COPASI—a COmplex PAthway SImulator. *Bioinformatics* **2006**, *22*, 3067−3074.

(12) Huang, Y.-T.; Wang, W.-C.; Hsu, C.-P.; Lu, W.-Y.; Chuang, W.-J.; Chiang, M. Y.; Lai, Y.-C.; Chen, H.-Y. The ring-opening polymerization of ε-caprolactone and l-lactide using aluminum complexes bearing benzothiazole ligands as catalysts. *Polym. Chem.* **2016**, *7*, 4367−4377.

(13) Zhang, Y.; Gao, A.; Zhang, Y.; Xu, Z.; Yao, W. Aluminum complexes with benzoxazolphenolate ligands: Synthesis, characterization and catalytic properties for ring-opening polymerization of cyclic esters. *Polyhedron* **2016**, *112*, 27−33.

(14) The M06-2X/6-311+G(d,p)//M06-L/6-31+G(d,p) level (including continuum toluene solvation effects) was chosen based on the prior excellent performance of this level of theory for rationalizing experimental trends in caprolactone polymerization catalyzed by aluminum coordination compounds as documented in refs 2a−2c.

(15) Frisch, M. J.; Trucks, G. W.; Schlegel, H. B.; Scuseria, G. E.; Robb, M. A.; Cheeseman, J. R.; Scalmani, G.; Barone, V.; Mennucci, B.; Petersson, G. A.; et al. *Gaussian 09*, revision E.01; Gaussian, Inc.: Wallingford, CT, 2009.

(16) Zhao, Y.; Truhlar, D. G. The M06 Suite of Density Functionals for Main Group Thermochemistry, Thermochemical Kinetics, Noncovalent Interactions, Excited States, and Transition Elements: Two New Functionals and Systematic Testing of Four M06-Class Functionals and 12 Other Functionals. *Theor. Chem. Acc.* **2008**, *120*, 215−241.

(17) Hehre, W. J.; Ditchfield, R.; Pople, J. A. Self-Consistent Molecular Orbital Methods. XII. Further Extensions of Gaussian-Type Basis Sets for Use in Molecular Orbital Studies of Organic Molecules. *J. Chem. Phys.* **1972**, *56*, 2257−2261.

(18) Krishnan, R.; Binkley, J. S.; Seeger, R.; Pople, J. A. Self-Consistent Molecular Orbital Methods. XX. A Basis Set for Correlated Wave Functions. *J. Chem. Phys.* **1980**, *72*, 650−654.

(19) Marenich, A. V.; Cramer, C. J.; Truhlar, D. G. Universal Solvation Model Based on Solute Electron Density and on a Continuum Model of the Solvent Defined by the Bulk Dielectric Constant and Atomic Surface Tensions. *J. Phys. Chem. B* **2009**, *113*, 6378−6396.

(20) For completeness, we note that the predicted free energy for the final product along the reaction coordinate in Figure 5 for the TMTAA ligand is 7.8 kcal/mol; i.e., the overall reaction is predicted to be endergonic. While part of this may be associated with initiation being less favorable than polymerization, another significant issue is the underestimation of the entropy of a growing polymer chain when computed simply from application of the conventional ideal-gas, rigid-rotator, harmonic-oscillator approximation to a single product structure, as previously also discussed in the following: (a) Martinez, H.; Miró, P.; Charbonneau, P.; Hillmyer, M. A.; Cramer, C. J. Selectivity in Ring-opening Metathesis Polymerization of Z-Cyclooctenes Catalyzed by a Second-generation Grubbs Catalyst. *ACS Catal.* **2012**, *2*, 2547−2556. (b) Martinez, H.; Hillmyer, M. A.; Cramer, C. J. Factors Controlling the Regio- and Stereoselectivity of the Ring-Opening Metathesis Polymerization of 3-Substituted Cyclooctenes by Monoaryloxide Pyrrolide Imido Alkylidene (MAP) Tungsten Catalysts. *J. Org. Chem.* **2014**, *79*, 11940−11948.

DOI: 10.1021/acs.inorgchem.6b02849
Inorg. Chem. 2017, 56, 725−728